Title

Invading cancer cells are predominantly in G0/G1 resulting in chemoresistance demonstrated by real-time FUCCI imaging

Journal

Cell Cycle, 13(6)

ISSN

1538-4101

Authors

Yano, Shuya
Miwa, Shinji
Mii, Sumiyuki
et al.

Publication Date

2014-03-15

DOI

10.4161/cc.27818

Peer reviewed

Cell Cycle 13:6, 953–960; March 15, 2014; © 2014 Landes Bioscience

Invading cancer cells are predominantly in G_0/G_1 resulting in chemoresistance demonstrated by real-time FUCCI imaging

Shuya Yano[1,2,3], Shinji Miwa[1,2], Sumiyuki Mii[1,2], Yukihiko Hiroshima[1,2], Fuminari Uehara[1,2], Mako Yamamoto[1,2], Hiroyuki Kishimoto[3], Hiroshi Tazawa[4], Michael Bouvet[2], Toshiyoshi Fujiwara[3], and Robert M Hoffman[1,2,*]

[1]AntiCancer, Inc; San Diego, CA USA; [2]Department of Surgery; University of California, San Diego; San Diego, CA USA; [3]Department of Gastroenterological Surgery; Okayama University Graduate School of Medicine, Dentistry, and Pharmaceutical Sciences; Okayama, Japan; [4]Center for Innovative Clinical Medicine; Okayama University Hospital; Okayama, Japan

Keywords: cancer invasion, cell cycle kinetics, fluorescent proteins, FUCCI, 3D, Gelfoam® histoculture, confocal laser microscopy, real-time imaging

Abbreviations: FUCCI, fluorescence ubiquitination cell cycle indicator; CLSM, confocal laser scanning microscopy

Invasive cancer cells are a critical target in order to prevent metastasis. In the present report, we demonstrate real-time visualization of cell cycle kinetics of invading cancer cells in 3-dimensional (3D) Gelfoam® histoculture, which is in vivo-like. A fluorescence ubiquitination cell cycle indicator (FUCCI) whereby G_0/G_1 cells express a red fluorescent protein and $S/G_2/M$ cells express a green fluorescent protein was used to determine the cell cycle position of invading and non-invading cells. With FUCCI 3D confocal imaging, we observed that cancer cells in G_0/G_1 phase in Gelfoam® histoculture migrated more rapidly and further than cancer cells in $S/G_2/M$ phases. Cancer cells ceased migrating when they entered $S/G_2/M$ phases and restarted migrating after cell division when the cells re-entered G_0/G_1. Migrating cancer cells also were resistant to cytotoxic chemotherapy, since they were preponderantly in G_0/G_1, where cytotoxic chemotherapy is not effective. The results of the present report suggest that novel therapy targeting G_0/G_1 cancer cells should be developed to prevent metastasis.

Introduction

Cancer cell invasion is the prelude for metastasis.[1-3] Therefore, targeting invading cancer cells is critical to prevent metastasis.[4-6] However, in order to target invading cancer cells, it is necessary to determine their cell cycle phase, since most cytotoxic chemotherapy targets $S/G_2/M$ cells. Sakaue-Sawano et al.[7] have utilized oscillating proteins that specifically mark cell cycle phases in order to image cell cycle kinetics in a system they term FUCCI (fluorescence ubiquitination cell cycle indicator). Individual G_1 phase nuclei are red, and those in $S/G_2/M$ phases are green in the FUCCI system.

For tracking invading cancer cells, 3-dimensional culture is indispensable.[8-12] Collagen sponge-gel histoculture was developed by Leighton.[13] Placing cells in histoculture enables them to form 3-dimensional structures.[13] Because of its architectural resemblance to native tissue, sponge gel histoculture represents a unique in vivo-like model to study cancer-cell behavior.[14] For example, Leighton observed that when C3HBA mouse mammary adenocarcinoma cells were grown on sponge-matrix histoculture, the cells aggregated similar to the original in vivo tumor. Distinct structures were formed within the tumors, such as lumina and stromal elements, with some of the glandular structures similar to the original tumor. When Leighton cultured hepatoma cells in sponge-matrix culture, they behaved differently from the normal liver cells and grew in a loosely packed arrangement as opposed to normal liver cells.[15]

We have further developed sponge gel histoculture using Gelfoam® to grow tumors,[16,17] nerves growing from stem cells,[18-20] hair follicles,[21] skin with growing hair,[22] and Margolis et al.[23] have used Gelfoam® to culture lymphoid tissue.

In the present report, we use confocal imaging and Gelfoam® collagen sponge gel histoculture of human stomach cancer cells expressing FUCCI to determine the cell cycle position of invasive and non-invasive cancer cells and their sensitivity to cytotoxic chemotherapy. The implication of these results for the study and treatment of metastasis are discussed.

*Correspondence to: Robert M Hoffman; Email: all@anticancer.com
Submitted: 12/19/2013; Accepted: 01/12/2014; Published Online: 01/20/2014
http://dx.doi.org/10.4161/cc.27818

Results and Discussion

Gelfoam® 3-dimensional histoculture enables real-time tracking of FUCCI-expressing invading and non-invading cancer cells

In Gelfoam® histoculture, invading cancer cells were mostly in G_0/G_1 phase, while non-invading cells were mostly in $S/G_2/M$ phases (**Fig. 1A**). The cell cycle distribution of invading cells was 84.3% in G_0/G_1 phase. In contrast, in non-invading cells at the tumor surface, the percentage of cells in $S/G_2/M$ was 67.5% (**Fig. 1A**). Cancer cells located at the invading area of a Gelfoam® tumor could be tracked for at least 3 days (**Fig. 1B; Video S1**). Some invading cancer cells migrated along the structure of the Gelfoam® (**Fig. 1C; Video S1**); the other cancer cells spread inside the structure of the Gelfoam® (**Fig. 1C; Video S1**).

Cell cycle distribution of the invading versus non-invading areas of tumors in Gelfoam® histoculture

Cancer cells at the invading edge of the tumor moved along the Gelfoam® structures and were mostly in G_0/G_1 (94.0 ± 4.9%) (**Fig. 2A**). In contrast, cancer cells at the center of the tumor fluoresced red, yellow, and green and were thus distributed throughout the cell cycle (S phase; 23.7 ± 18.0%; G_2/M phase; 30.5 ± 16.6%) (**Fig. 2A**). Cancer cells in G_0/G_1 phase contacted each other (**Fig. 2B**).

Cancer cells in G_0/G_1-phase are motile compared with $S/G_2/M$-phase cancer cells in Gelfoam® histoculture

Cancer cells in G_0/G_1 phase migrated more than cancer cells in $S/G_2/M$ at the tumor edge in Gelfoam®: G_0/G_1 phase, 66.5 ± 31.2 μm/48 h; $S/G_2/M$ phase, 21.8 ± 14.0 μm/48 h; $P < 0.0001$ (**Fig. 3A, C, and D**). Moreover, single cancer cells in G_0/G_1 phase migrated significantly further (up to 200 μm over 48 h) than those in $S/G_2/M$ phases (up to 90 μm over 48 h) (**Fig. 3B and D; Video S2**).

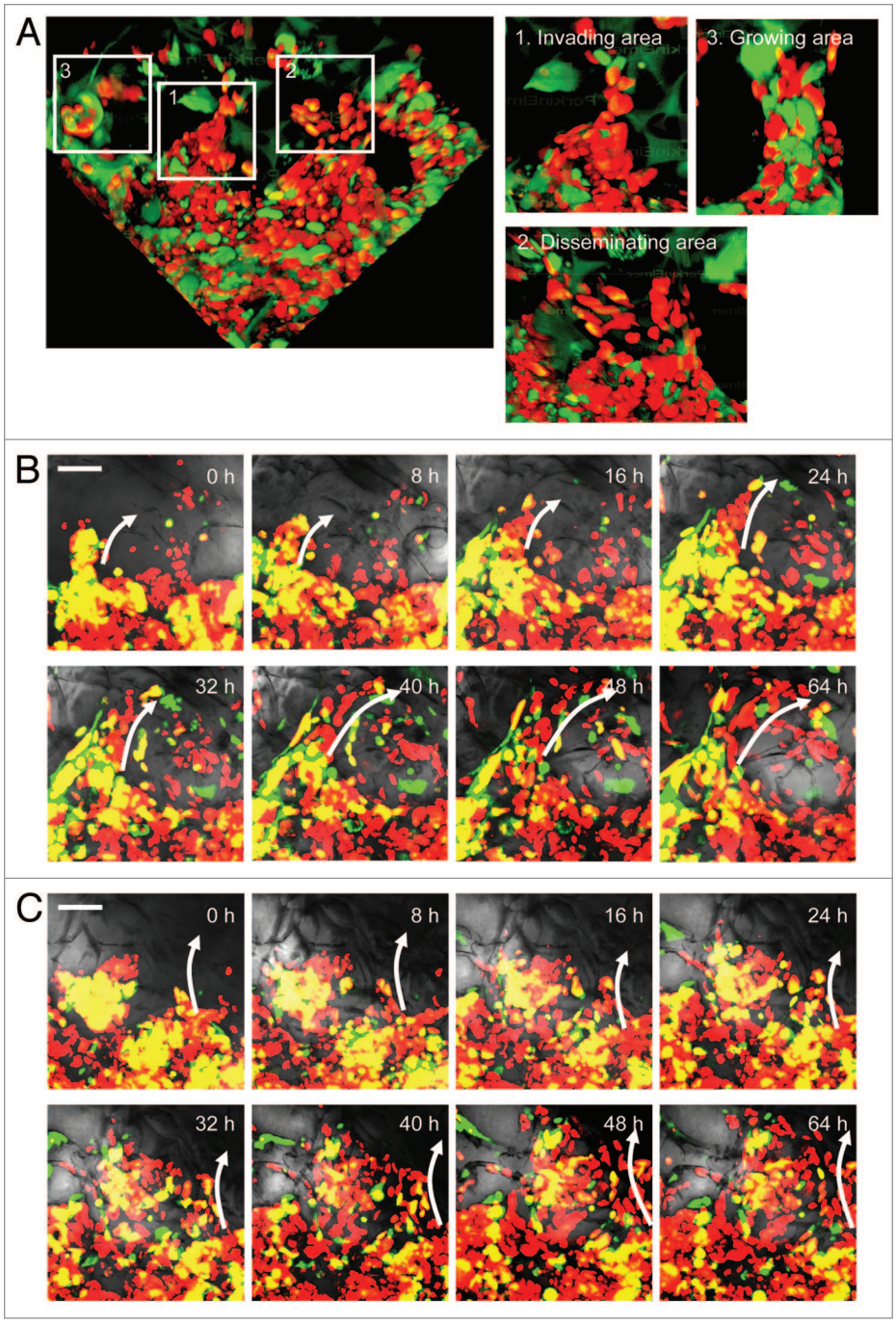

Figure 1. Gelfoam® histoculture enables tracking of the cell cycle kinetics of invading and non-invading FUCCI-expressing cancer cells. All images were acquired with confocal laser scanning microscopy (CLSM) using the FV1000 (Olympus). FUCCI-expressing cancer cells in G_0/G_1, S, or G_2/M phases appear red, yellow, or green, respectively. FUCCI-expressing cancer cells (2×10^7) were placed on Gelfoam® (1 × 1 cm) in RPMI 1640 medium. (**A**) Gelfoam® culture enables cancer cells to be visualized at different locations in tumor-like structures (left). High magnification view (right). (**B**) High-magnification real-time images of cancer cells invading from a tumor on Gelfoam® for 64 h. Arrows show the direction of invading cancer cells. (**C**) High-magnification real-time images of cancer cells disseminating from a tumor on Gelfoam® for 64 h. Arrows show the direction of invading cancer cells. Scale bars: 100 μm.

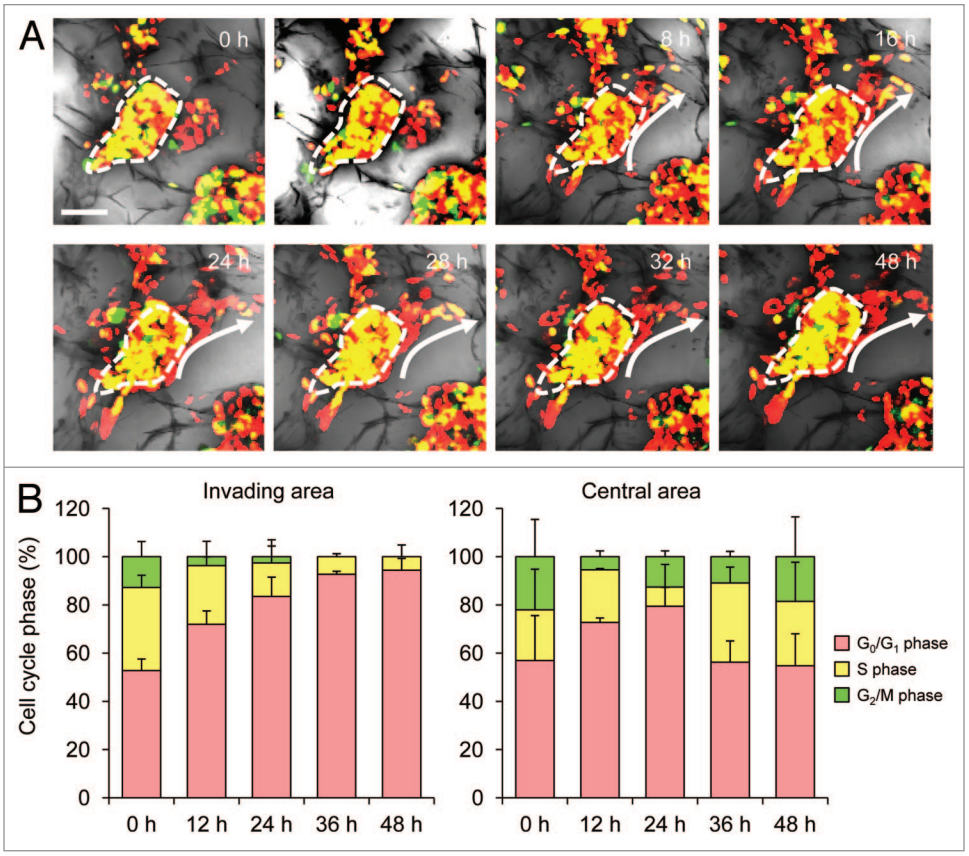

Figure 2. Cell cycle distribution of invasive and noninvasive cancer cells. FUCCI-expressing cancer cells (1×10^7) were placed on Gelfoam® (1×1 cm) in RPMI 1640 medium. (**A**) High-magnification real-time images of a small tumor growing on Gelfoam® for 48 h. Arrows show the direction of invading cancer cells. Dashed lines show the non-invading area. (**B**) Histogram of cell cycle distribution of invading area and central non-invading area of a tumor growing on Gelfoam®. Scale bar: 100 μm.

Cancer cells in G_0/G_1 phase migrate faster than cancer cells in $S/G_2/M$ phases in Gelfoam® histoculture

Real-time confocal imaging of single-cell movement from the edge of tumors growing in Gelfoam® was performed. Cancer cells in G_0/G_1 phase migrated more rapidly than cancer cells in $S/G_2/M$ phases. The velocity of G_0/G_1 phase cells was 1.46 ± 0.44 μm/h. In contrast, the velocity of $S/G_2/M$-phase cells was 0.11 ± 0.014 μm/h ($P = 0.006$) (**Fig. 4A–C**).

Cancer cells in G_0/G_1 phase cease migration upon entry in $S/G_2/M$ phases and restart migration after cell division and re-entry in G_0/G_1 in Gelfoam® histoculture

When migrating cancer cells in G_0/G_1 phase subsequently cycled into $S/G_2/M$ phases, they ceased migration (**Fig. 5A; Video S3**). When the cancer cells re-entered G_0/G_1, they began to migrate again (**Fig. 5A; Video S3**).

Thirty G_0/G_1 cells were followed for 66 h. Some of the G_1/G_0 cells cycled into $S/G_2/M$ phases, where they stopped migrating and then divided and cycled into G_0/G_1. These cells were followed for an additional 24 h, during which time they migrated approximately 100 μm (**Fig. 5B**).

Cancer cells in G_0/G_1 phase can attach to Gelfoam® and invade more rapidly than those in S/G_2 phase

Real-time imaging of the behavior of a cell suspension layered on Gelfoam® showed that cancer cells in G_0/G_1 phase attached to Gelfoam® and began invading more rapidly (16.7 ± 8 h) than cancer cells in $S/G_2/M$ phases (30.0 ± 8 h) ($P = 0.0026$) (**Fig. 6A–C; Video S4**).

Chemotherapy does not kill or inhibit the movement of invading G_0/G_1 cancer cells in Gelfoam® histoculture

Cisplatinum (25 μm) effectively killed cancer cells in $S/G_2/M$ phases (85.0 ± 9.1% cells in apoptosis) (**Fig. 7A–E; Video S5**). In contrast, cisplatinum had little efficacy against cancer cells in G_0/G_1 phase (5.0 ± 5.9% cells in apoptosis) (**Fig. 7A–D**) and did not inhibit their movement (**Fig. 7E; Video S5**). These findings indicated that invading cancer cells in G_0/G_1 phase are resistant to cisplatinum.

In the present report, we compared the cell cycle dynamics of invading and non-invading cancer cells in 3-dimensional Gelfoam® histoculture, where cancer cells have in vivo-like behavior. Real-time imaging of cell cycle kinetics was made possible

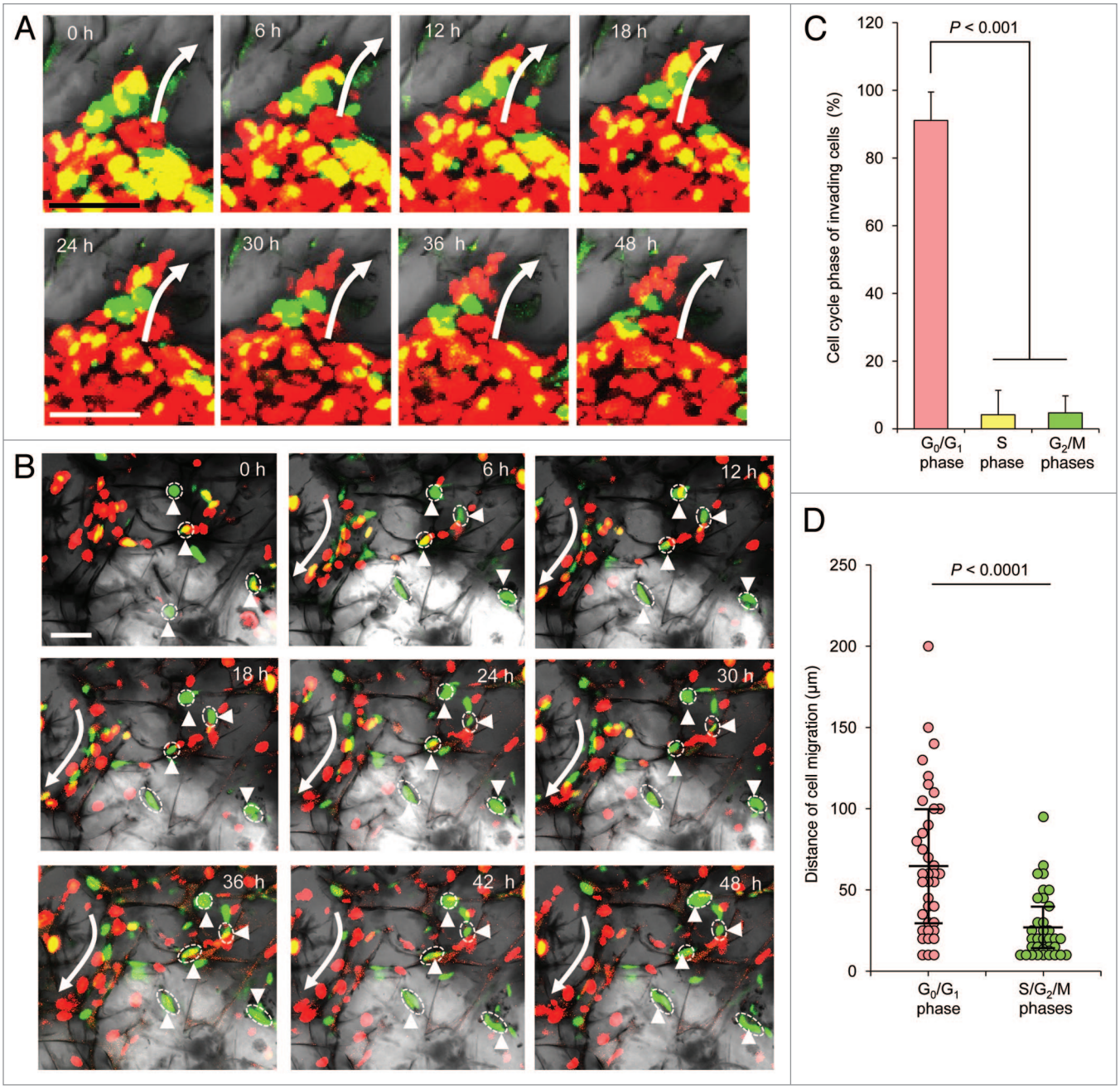

Figure 3. Invasive cancer cells are predominantly in G_0/G_1. FUCCI-expressing cancer cells (5×10^6) were placed on Gelfoam® (1 × 1 cm) in RPMI 1640 medium. (**A**) High-magnification real-time images of invading cancer cells cultured on Gelfoam® for 48 h. Arrows show the direction of invading cancer cells. (**B**) High-magnification real-time images of cancer cells in G_0/G_1 phase and in $S/G_2/M$ phases. Arrows show the direction of invading cancer cells. The cells circled with white dashed lines and pointed by arrowheads are non-invading cells. (**C**) Histogram shows cell cycle phase of invading cancer cells. (**D**) Scatter diagram shows the distance cancer cells migrated in G_0/G_1 phase compared with cancer cells in $S/G_2/M$ phases. Scale bars: 100 μm.

with the use of FUCCI-expressing cancer cells. We demonstrated that cancer cells in G_0/G_1 phase can migrate faster and further than cancer cells in $S/G_2/M$ phases. When cancer cells in G_0/G_1 cycled into $S/G_2/M$ phases, they ceased movement and then only restarted migration after re-entry into G_0/G_1 phase after cell division. Chemotherapy had little effect on G_0/G_1 invading cancer cells. The results of the present report may explain, in part, why cytotoxic chemotherapy has limited efficacy to prevent metastasis.

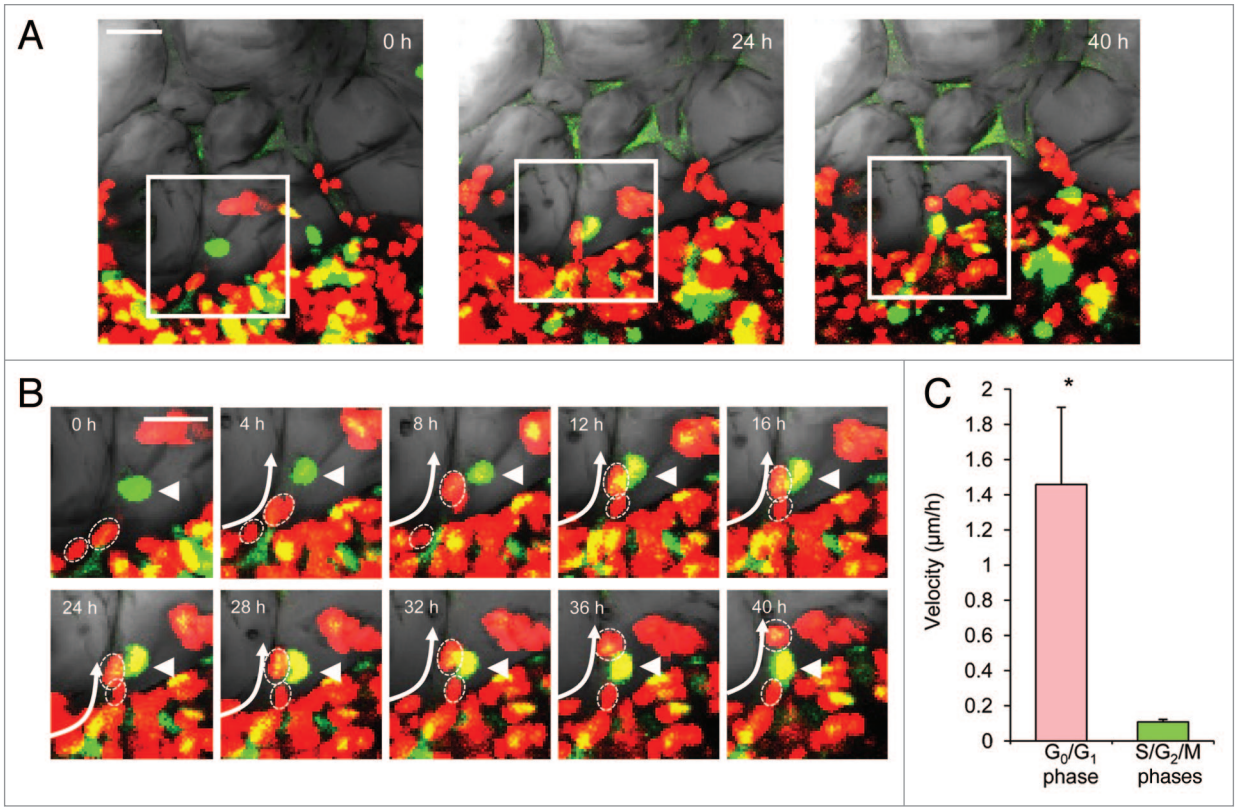

Figure 4. Behavior of individual FUCCI-expressing cancer cells cultured on Gelfoam®. FUCCI-expressing cancer cells (5×10^6) were placed on Gelfoam® (1×1 cm) in RPMI 1640 medium. (**A**) Low-magnification image of an overview of cancer cells cultured on Gelfoam® for 0 h, 24 h, or 40 h. (**B**) High-magnification real-time images of cancer cells in G_0/G_1 phase or in $S/G_2/M$ phases cultured on Gelfoam® for 48 h. Arrows show the direction of invading cancer cells. Circles with dashed lines show invading cells in G_0/G_1 phase. Arrowheads show a single non-invading cell. (**C**) Histogram shows the velocity of cancer cells in G_0/G_1 phase and $S/G_2/M$ phases. Scale bars: 50 μm.

Materials and Methods

Cells

MKN45 is a radio-resistant poorly differentiated stomach adenocarcinoma cell line derived from a liver metastasis of a patient.[24] The cells were grown in RPMI 1640 with 10% fetal bovine serum and penicillin/streptomycin.

Establishment of MKN45 cells stably transfected with FUCCI plasmids

Plasmids expressing mKO2-hCdt1 (green fluorescent protein) and mAG-hGem (orange fluorescent protein) were obtained from the Medical and Biological Laboratory.[7] Plasmids expressing mKO2-hCdt1 were transfected into MKN45 cells using Lipofectamine™ LTX (Invitrogen). The cells were incubated for 48 h after transfection and were then trypsinized and seeded in 96-well plates at a density of 10 cells/well. In the first step, cells were sorted for green fluorescence (S, G_2, and M phases) using a FACSAria cell sorter (Becton Dickinson). The first-step-sorted green-fluorescent cells were then super-transfected with mAG-hGem (orange) and then further sorted by orange fluorescence.

Cell culture

FUCCI-expressing MKN45 cells were seeded on plastic plates for 2-dimensional culture in RPMI-1640 medium (Mediatech). For 3-dimensional culture, FUCCI-expressing cells were cultured on Gelfoam® in the same medium.

Imaging of MKN45 cells expressing cell cycle-dependent fluorescent proteins

Confocal laser scanning microscopy was performed with the FV1000 confocal laser scanning microscopy (Olympus Corp.) with 2 laser diodes (473 nm and 559 nm). A 4× (0.20 numerical aperture immersion) objective lens and a 20× (0.95 numerical aperture immersion) objective lens (Olympus) were used. Scanning and image acquisition were controlled by Fluoview software (Olympus).[25] The tracing data were imported to Velocity 6.0 version (Perkin Elmer), where all 3D analysis was performed.

Statistical analysis

Data are shown as means ± SD. For comparison between 2 groups; significant differences were determined using the Student *t* test. *P* values of < 0.05 are considered significant.

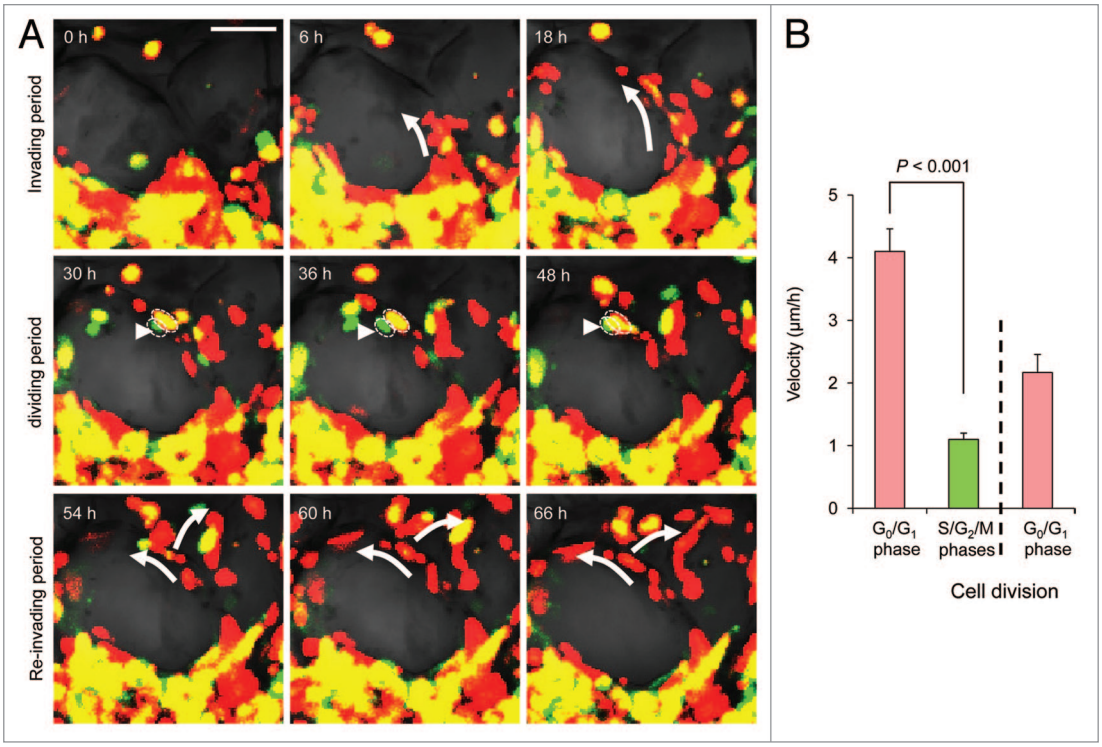

Figure 5. Comparison of migration velocity of cancer cells in G_0/G_1 phase and $S/G_2/M$ phases during cell division. FUCCI-expressing cancer cells (5×10^6) were placed on Gelfoam® (1×1 cm) in RPMI 1640 medium. (**A**) Cancer cells in G_0/G_1 phase migrated and subsequently cycled to $S/G_2/M$ phases. Arrows show the direction of G_0/G_1 phase of cancer-cell migration. Arrowheads show the cancer cells after cycling to $S/G_2/M$ phases. The cells circled with white dashed lines and pointed by arrowheads are non-invading cells. (**B**) Histogram shows the velocity of cancer cells in G_0/G_1 phase and in $S/G_2/M$ phases. Scale bar: 100 μm.

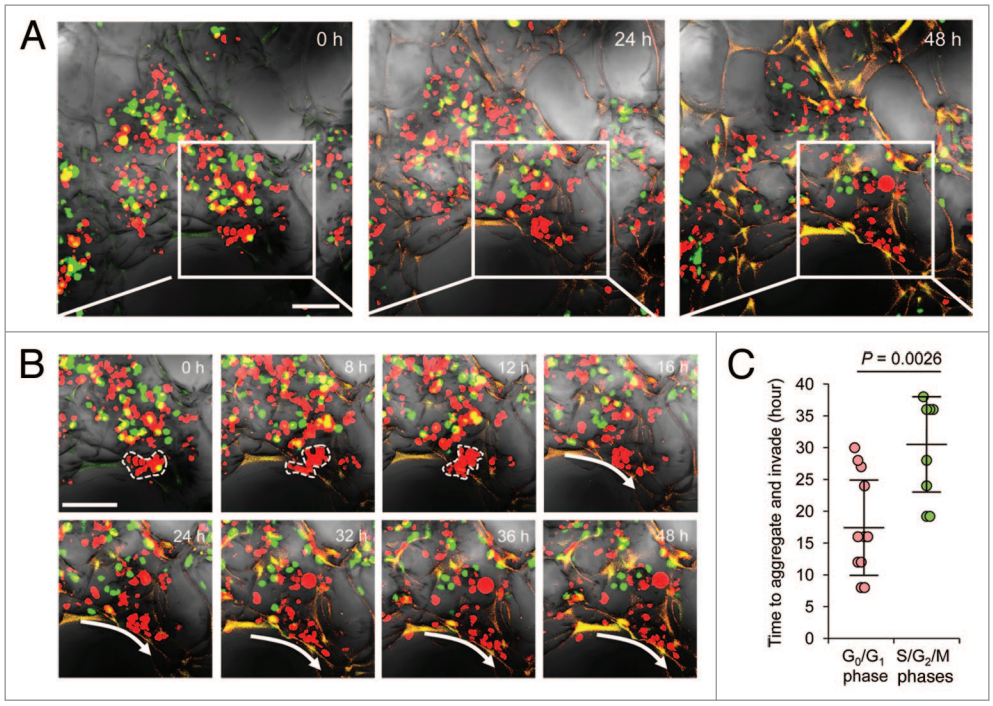

Figure 6. Cell cycle kinetics of cancer cells during seeding on Gelffoam®. FUCCI-expressing cancer cells (5×10^6) were placed on Gelfoam® (1×1 cm) in RPMI 1640 medium. (**A**) Low-magnification image of an overview of cancer cells cultured on Gelfoam® for 0 h, 24 h, or 48 h. (**B**) High-magnification real-time images of cancer cells in G_0/G_1 phase or in $S/G_2/M$ phases cultured on Gelfoam® for 48 h. Dashed lines show aggregating cells. Arrows show the direction of invading cancer cells. (**C**) Scatter diagram shows the number of hours to attach and invade taken by cancer cells in G_0/G_1 phase compared with $S/G_2/M$ phases. Scale bars: 100 μm.

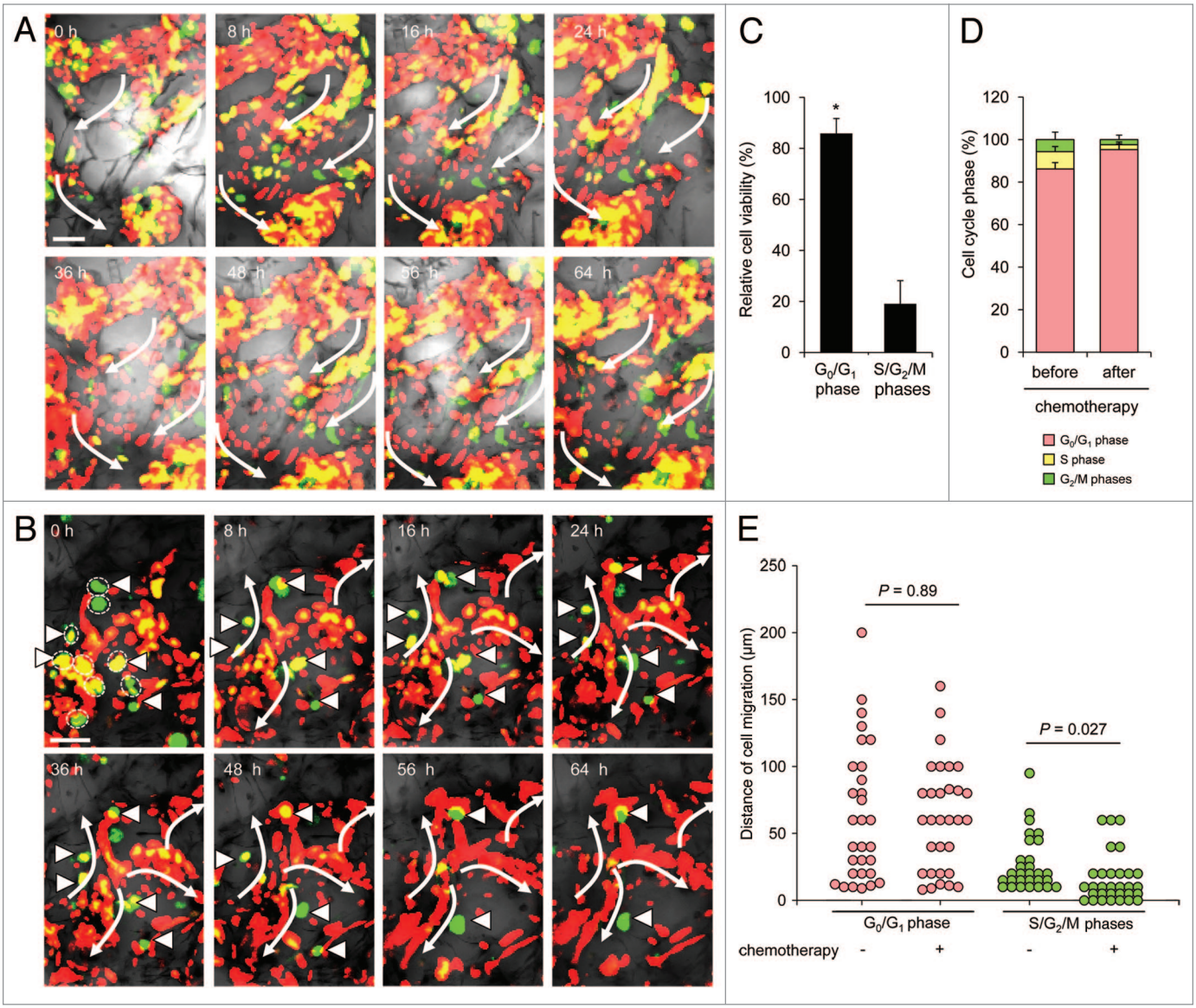

Figure 7. Chemotherapy does not kill or inhibit the movement of single invading cancer cells in G_0/G_1 phase. FUCCI-expressing cancer cells (2×10^6) were placed on Gelfoam® (1 × 1 cm) in RPMI 1640 medium. Three days after seeding, cisplatinum (25 μM) was added. (**A and B**) High-magnification real-time images of the disseminating area of a tumor for a 64 h period without (**A**) and with cisplatinum treatment (**B**). Arrows show the direction of invading cancer cells. The cells circled with white dashed lines and/or pointed by arrowheads are dying non-invading cells. (**C**) Histogram shows the survival rate of cancer cells in G_0/G_1 phase and $S/G_2/M$ phases 64 h after cisplatinum treatment. (**D**) Histogram shows the cell cycle distribution of cancer cells before and after cisplatinum treatment. (**E**) Scatter diagram shows the distance cancer cells migrated in G_0/G_1 phase and $S/G_2/M$ phases with or without chemotherapy. Scale bars: 100 μm.

Disclosure of Potential Conflicts of Interest

No potential conflicts of interest were disclosed.

Acknowledgments

This work was supported in part by National Cancer Institute grant CA132971.

Dedication

This paper is dedicated to the memory of A.R. Moossa, MD.

Author Contributions

S.Y. and R.M.H. conceived the idea for this project. S.Y. and R.M.H. designed all experiments and wrote the manuscript. S.Y., S.M., S.M., and M.Y. performed all experiments. H.K., H.T., M.B., and T.F. provided crucial ideas and helped with data interpretation. Y.H., F.U., and H.T. provided special technical assistance.

Supplemental Materials

Supplemental materials may be found at:
www.landesbioscience.com/journals/cc/article/27818

References

1. Chambers AF, Groom AC, MacDonald IC. Dissemination and growth of cancer cells in metastatic sites. Nat Rev Cancer 2002; 2:563-72; PMID:12154349; http://dx.doi.org/10.1038/nrc865
2. Sahai E. Illuminating the metastatic process. Nat Rev Cancer 2007; 7:737-49; PMID:17891189; http://dx.doi.org/10.1038/nrc2229
3. Lauffenburger DA, Horwitz AF. Cell migration: a physically integrated molecular process. Cell 1996; 84:359-69; PMID:8608589; http://dx.doi.org/10.1016/S0092-8674(00)81280-5
4. Goss PE, Chambers AF. Does tumour dormancy offer a therapeutic target? Nat Rev Cancer 2010; 10:871-7; PMID:21048784; http://dx.doi.org/10.1038/nrc2933
5. Aguirre-Ghiso JA. Models, mechanisms and clinical evidence for cancer dormancy. Nat Rev Cancer 2007; 7:834-46; PMID:17957189; http://dx.doi.org/10.1038/nrc2256
6. Gottesman MM. Mechanisms of cancer drug resistance. Annu Rev Med 2002; 53:615-27; PMID:11818492; http://dx.doi.org/10.1146/annurev.med.53.082901.103929
7. Sakaue-Sawano A, Kurokawa H, Morimura T, Hanyu A, Hama H, Osawa H, Kashiwagi S, Fukami K, Miyata T, Miyoshi H, et al. Visualizing spatiotemporal dynamics of multicellular cell cycle progression. Cell 2008; 132:487-98; PMID:18267078; http://dx.doi.org/10.1016/j.cell.2007.12.033
8. Abbott A. Cell culture: biology's new dimension. Nature 2003; 424:870-2; PMID:12931155; http://dx.doi.org/10.1038/424870a
9. Jacks T, Weinberg RA. Taking the study of cancer cell survival to a new dimension. Cell 2002; 111:923-5; PMID:12507419; http://dx.doi.org/10.1016/S0092-8674(02)01229-1
10. Friedl P, Alexander S. Cancer invasion and the microenvironment: plasticity and reciprocity. Cell 2011; 147:992-1009; PMID:22118458; http://dx.doi.org/10.1016/j.cell.2011.11.016
11. Friedl P, Sahai E, Weiss S, Yamada KM. New dimensions in cell migration. Nat Rev Mol Cell Biol 2012; 13:743-7; PMID:23072889; http://dx.doi.org/10.1038/nrm3459
12. Cukierman E, Pankov R, Stevens DR, Yamada KM. Taking cell-matrix adhesions to the third dimension. Science 2001; 294:1708-12; PMID:11721053; http://dx.doi.org/10.1126/science.1064829
13. Leighton J. A sponge matrix method for tissue culture; formation of organized aggregates of cells in vitro. J Natl Cancer Inst 1951; 12:545-61; PMID:14889259
14. Leighton J. The growth patterns of some transplantable animal tumors in sponge matrix tissue culture. J Natl Cancer Inst 1954; 15:275-93; PMID:13233883
15. Leighton J, Justh G, Esper M, Kronenthal RL. Collagen-coated cellulose sponge: three dimensional matrix for tissue culture of Walker tumor 256. Science 1967; 155:1259-61; PMID:6018647; http://dx.doi.org/10.1126/science.155.3767.1259-a
16. Freeman AE, Hoffman RM. In vivo-like growth of human tumors in vitro. Proc Natl Acad Sci USA 1986; 83:2694-8; PMID:3458228; http://dx.doi.org/10.1073/pnas.83.8.2694
17. Hoffman RM. Tissue Culture. In: Brenner's Encyclopedia of Genetics, 2nd Ed., 2013; 7:73-6.
18. Mii S, Duong J, Tome Y, Uchugonova A, Liu F, Amoh Y, Saito N, Katsuoka K, Hoffman RM. The role of hair follicle nestin-expressing stem cells during whisker sensory-nerve growth in long-term 3D culture. J Cell Biochem 2013; 114:1674-84; PMID:23444061; http://dx.doi.org/10.1002/jcb.24509
19. Mii S, Uehara F, Yano S, Tran B, Miwa S, Hiroshima Y, Amoh Y, Katsuoka K, Hoffman RM. Nestin-expressing stem cells promote nerve growth in long-term 3-dimensional gelfoam®-supported histoculture. PLoS One 2013; 8:e67153; PMID:23840607; http://dx.doi.org/10.1371/journal.pone.0067153
20. Mii S, Amoh Y, Katsuoka K, Hoffman RM. Comparison of nestin-expressing multipotent stem cells in the tongue fungiform papilla and vibrissa hair follicle. J Cell Biochem 2013; In press; PMID:24142339; http://dx.doi.org/10.1002/jcb.24696.
21. Duong J, Mii S, Uchugonova A, Liu F, Moossa AR, Hoffman RM. Real-time confocal imaging of trafficking of nestin-expressing multipotent stem cells in mouse whiskers in long-term 3-D histoculture. In Vitro Cell Dev Biol Anim 2012; 48:301-5; PMID:22580909; http://dx.doi.org/10.1007/s11626-012-9514-z
22. Li L, Margolis LB, Paus R, Hoffman RM. Hair shaft elongation, follicle growth, and spontaneous regression in long-term, gelatin sponge-supported histoculture of human scalp skin. Proc Natl Acad Sci USA 1992; 89:8764-8; PMID:1528891; http://dx.doi.org/10.1073/pnas.89.18.8764
23. Grivel JC, Ito Y, Fagà G, Santoro F, Shaheen F, Malnati MS, Fitzgerald W, Lusso P, Margolis L. Suppression of CCR5- but not CXCR4-tropic HIV-1 in lymphoid tissue by human herpesvirus 6. Nat Med 2001; 7:1232-5; PMID:11689888; http://dx.doi.org/10.1038/nm1101-1232
24. Yokozaki H. Molecular characteristics of eight gastric cancer cell lines established in Japan. Pathol Int 2000; 50:767-77; PMID:11107048; http://dx.doi.org/10.1046/j.1440-1827.2000.01117.x
25. Uchugonova A, Duong J, Zhang N, König K, Hoffman RM. The bulge area is the origin of nestin-expressing pluripotent stem cells of the hair follicle. J Cell Biochem 2011; 112:2046-50; PMID:21465525; http://dx.doi.org/10.1002/jcb.23122v